Comparison of Substructure Of Compacted/Vermicular Graphite with Other Types Of Graphite

H. Itofuji
Y. Kawano
S. Yamamoto
N. Inoyama
Kyoto University, Kyoto, Japan
H. Yoshida
Sumitomo Light Metal Ind. Ltd., Nagoya City, Japan
Chang
IIT Fer et Titane, Tokyo, Japan

ABSTRACT

The substructure of compacted/vermicular (C/V) graphite was studied and those of kish, flake and spheroidal graphite were also studied for comparison using a scanning-transmission electron microscopy (STEM).

It was observed with the scanning electron microscopy (SEM) that C/V graphite was interconnected similar to flake graphite, the formation mechanism was, however, similar to spheroidal graphite. Some spheroidal graphite connected with C/V graphite in the graphite cells were frequently observed.

The diffraction pattern was observed with the transmission electron microscopy (TEM) to study the crystallographic orientation on every graphite. The diffraction patterns showed that every type of graphite grew dominantly along a-axis of hexagonal graphite crystal, although spheroidal and C/V graphites grew along the c-axis of that in external appearance.

From the SEM and TEM photographs, it was observed that spheroidal and C/V graphite had the polycrystal form and are constructed of the graphite tips, of which plate is the basal plane. These tips are layered parallel to the graphite surface. Thus spheroidal and C/V graphite read basically the same substructure.

It has been concluded that every graphite form depends on the sites where they crystallize, because graphite grows dominantly along the a-axis everywhere it crystallizes.

INTRODUCTION

The formation process of C/V graphite has been made and its precipitation at the filmy melt channel has been predicted.[1] This paper reports on the substructure of C/V graphite. The substructure was studied to make sure how C/V graphite precipitates at filmy melt channels and to check the formation process on it. It is important to observe the graphite substructure because the nucleation and growth process are reflected in it and are predicted from its crystalline feature. Therefore many studies on the graphite substructure have been done to explain the graphite formation.

Loper[2,3] has reported that the crystal structure of C/V graphite is similar to that of spheroidal graphite and that the dominant macroscopic growth direction of the C/V graphite is nearly along the c-axis of the hexagonal graphite crystal, although the microscopic growth direction appears to be along the edge of basal planes. Aleksandrov[4] has reported that vermicular graphite particles consist of crystallite aggregates with different growth-plane orientation; the growth planes are almost concentric and growth takes place mainly on basal plane. Their studies, however, are based on the observation with SEM and optical microscopy. Therefore, their considerations may not be absolutely correct because they didn't consider crystallographic orientation based upon an electron diffraction pattern with TEM.

The authors have observed the substructure of C/V graphite and some other graphites for comparison, using electron microscopy mainly. Then the mechanism of nucleation and growth process of compacted C/V graphite has been considered from the SEM and TEM structures, and the diffraction patterns.

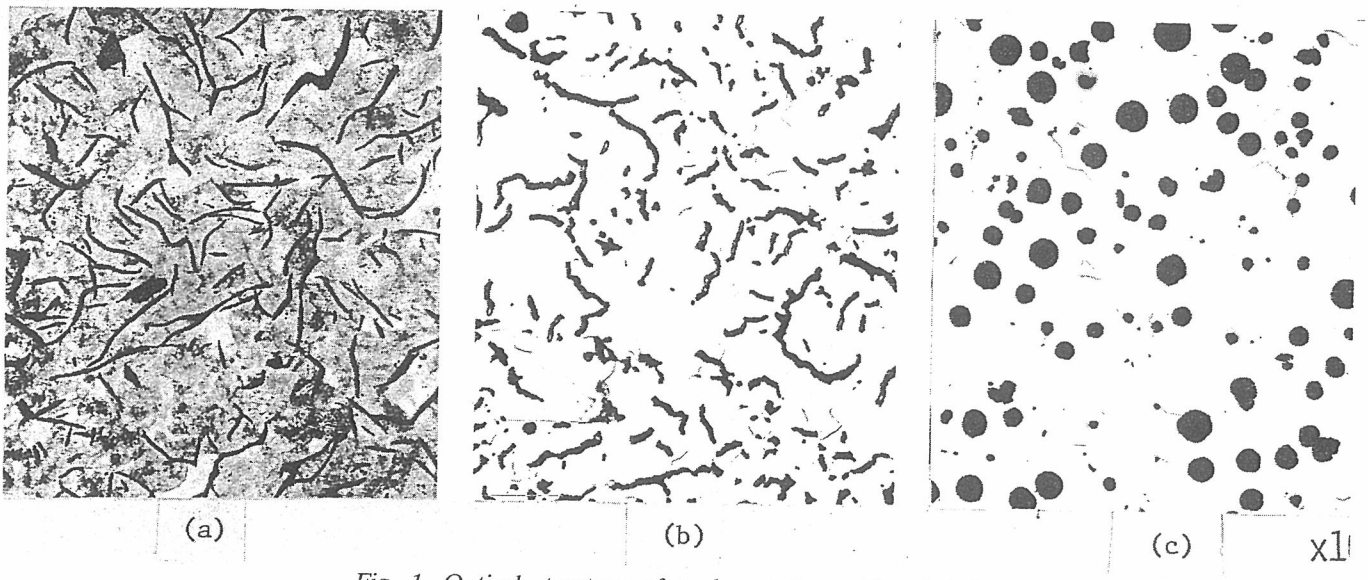

Fig. 1. Optical structure of each cast iron with: a) flake graphite; b) C/V graphite; c) spheroidal graphite. 2% Nital etch. (100X)

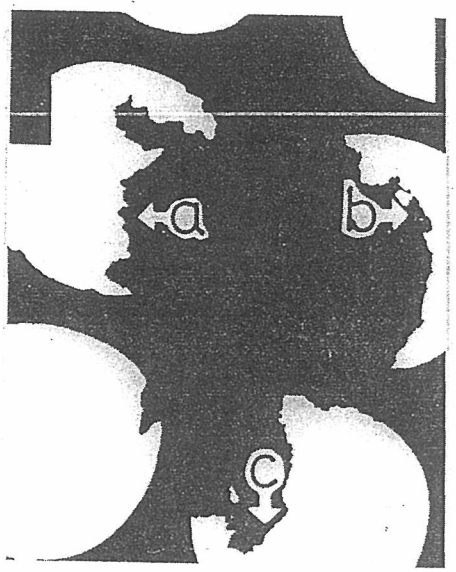

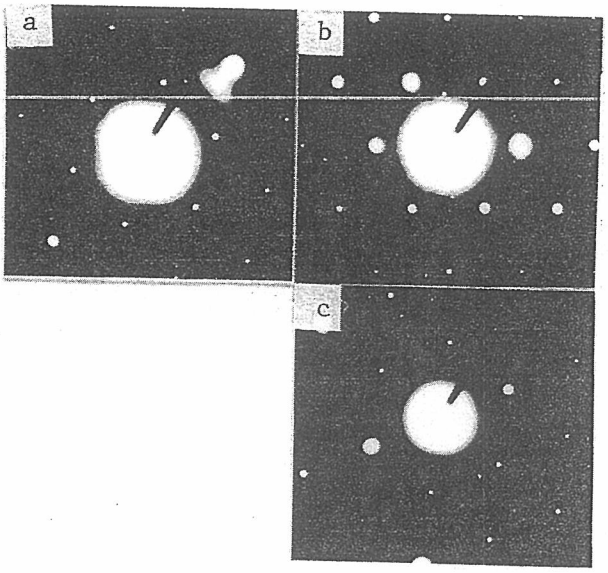

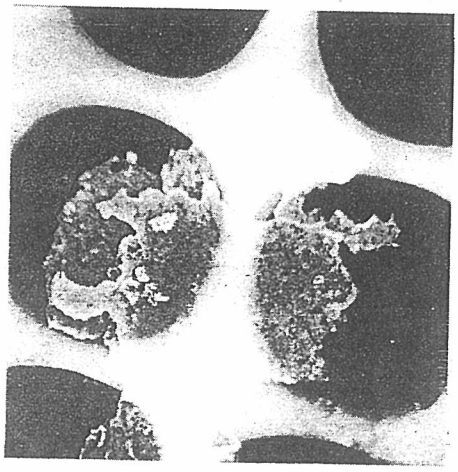

Fig. 2. TEM and SEM photograph and diffraction pattern of kish graphite.

EXPERIMENTAL PROCEDURE

Graphite substructures were observed, not only C/V graphite but also kish, flake and spheroidal graphite. The optical microscopic structures of each cast iron studied are presented in Fig. 1. It can be seen that all of them have typical graphite

Table 1. Chemical Composition of Each Base Metal and Treatment

	C	Si	Mn	P	S	Treatment
Flake graphite cast iron	3.43	1.95	0.01	0.002	0.011	———
C/V graphite cast iron	3.43	1.95	0.01	0.002	0.011	0.9% of 50%Ce mish metal
Spheroidal graphite cast iron	3.56	2.46	0.01	0.002	0.025	4% of Fe-Si-5.5%Mg

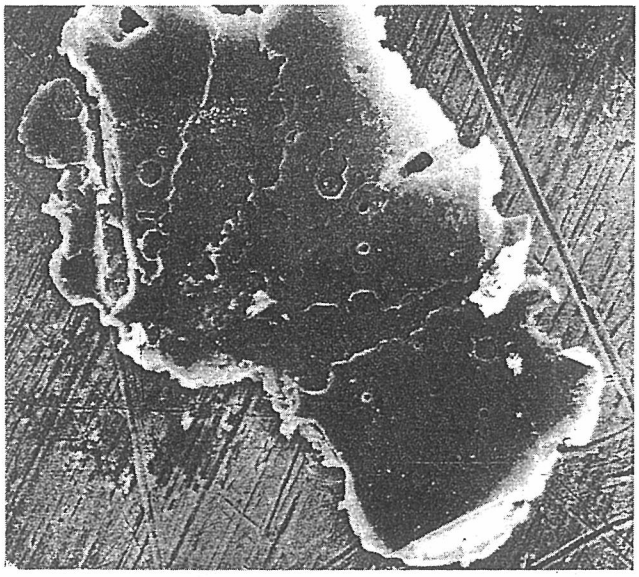

Fig. 3. SEM photograph of kish graphite. ×220

structures. The chemical composition of each base metal and the treatment for C/V graphite and SG cast irons are presented in Table 1. Graphites were electrolytically extracted from cast iron matrices. Kish graphite was, however, gathered around a cryptol electric furnace during melting hyper eutectic cast iron. Then the current density was set about $0.3A/cm^2$ and the electrolyte containing 15% sodium citrate, tribasic, 30% citric acid, 1.5% potassium bromaid and 53.5% water (pH = 3) was used. Then these graphites were repeatedly rinsed with 5% Na_2CO_3 aq and HCl + H_2O (1 + 10) before a final rinse with ethyl alcohol.

Then the graphite was put on the specimen grid with collodion film and it was set into electron microscopy. The SEM structure was observed at acceleration voltage of 40 kV, and the TEM structure and diffraction pattern were observed at acceleration voltage of 200 kV. When the stereo structure of graphite was needed, the secondary electron image (SEI) was taken with electron probe micro analyzer (EPMA) at acceleration voltage of 20 kV.

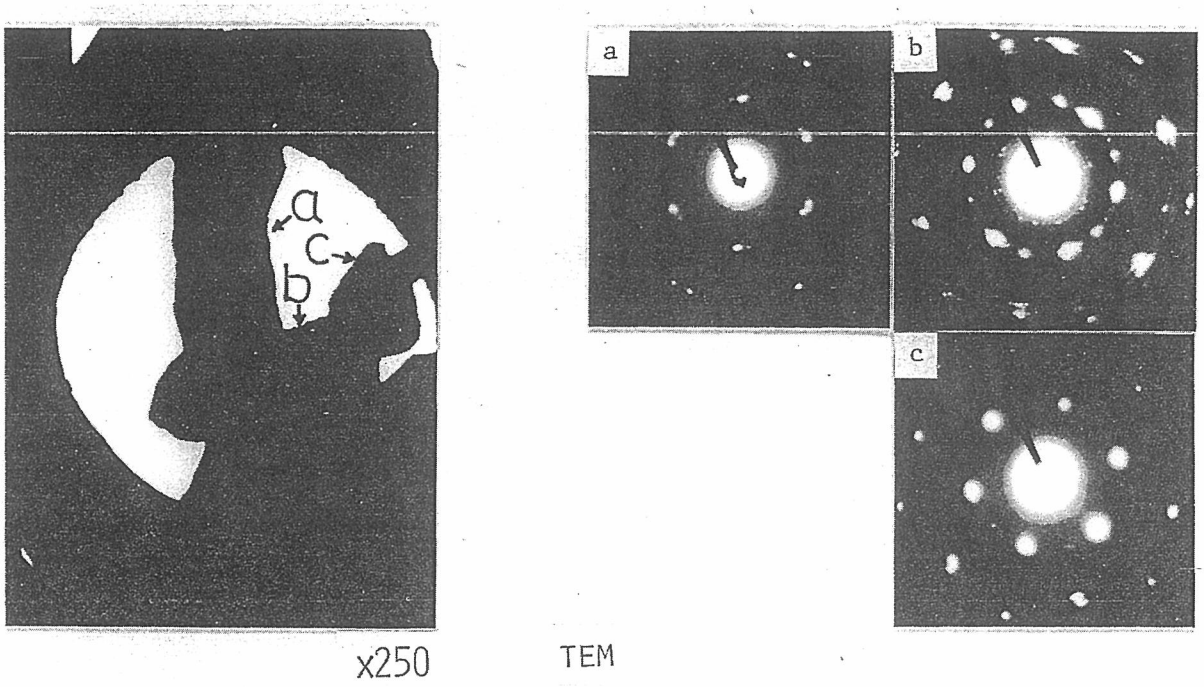

Fig. 4. TEM and SEM photograph and diffraction pattern of flake graphite.

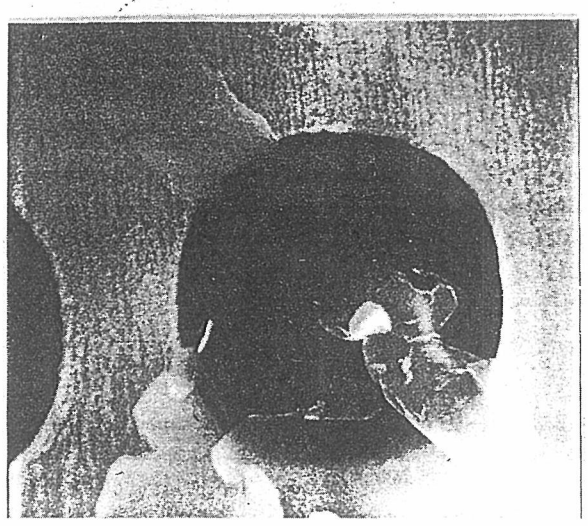

RESULTS AND DISCUSSION

Substructure of Kish Graphite

The SEM and TEM photograph and the diffraction pattern of kish graphite are presented in Fig. 2.

It is observed from SEM photograph that kish graphite is a plate without any branches and is constructed of layers of graphite plates. This is shown more clearly in Fig. 3, which was observed by EPMA with lower acceleration voltage. Each diffraction pattern in Fig. 2 shows that the plate surface of kish graphite is the basal plane.

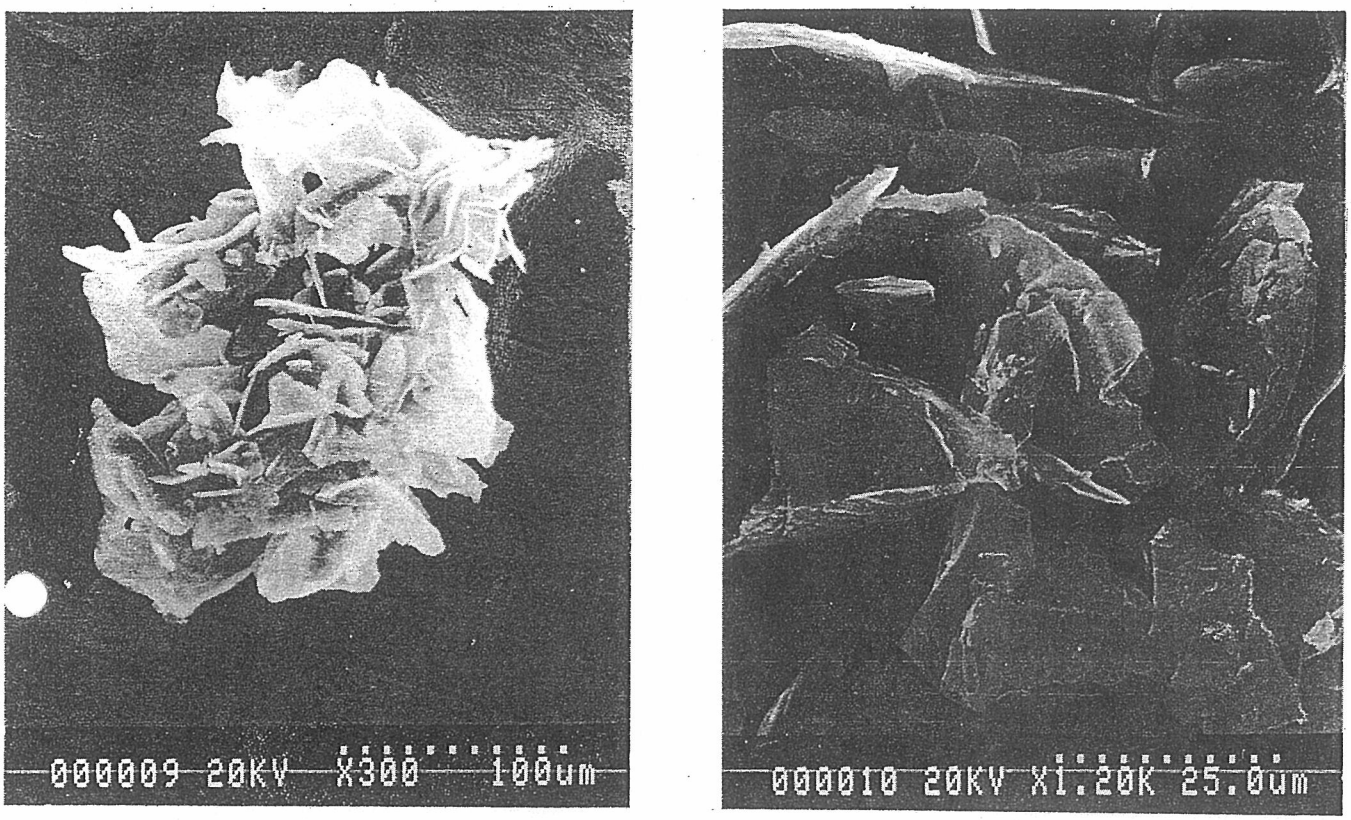

Fig. 5. SEM photograph of flake graphite.

From these factors, it may be sure that the dominant growth direction of kish graphite is the a-axis of the hexagonal graphite crystal.

Substructure of Flake Graphite

The TEM and SEM photograph and diffraction pattern of the s e flake graphite are presented in Fig. 4. It is observed from S M photograph that flake graphite is branched and has little thickness. The clearer photograph of flake graphite cell observed by EPMA (= electron probe x-ray micro analyzer) is presented in Fig. 5. The diffraction pattern shows twinings which is a rotation around the c-axis. Therefore it is evident that the plate surface of flake graphite is also the basal plane of the hexagonal graphite crystal. This means that the dominant growth direction of flake graphite is along the a-axis.

Substructure of Spheroidal Graphite

The SEM and TEM photograph and diffraction pattern of the same spheroidal graphite are presented in Fig. 6. The diffraction patterns were observed at points a ~ g shown in the TEM photograph. It is observed that all patterns indicate (002) spot. This means that the electron is applied parallel to the basal plane of the hexagonal graphite crystal and that the surface of spheroidal graphite is covered with basal plane. The direction of the c-axis is perpendicular to every surface.

The SEM photographs in Fig. 7 show that spheroidal graphite is constructed of graphite tips and these tips are layered parallel to the surface. It is sure from the diffraction patterns in Fig. 6 that the surface of the each tip is the basal plane. Thus it is obvious that spheroidal graphite has a polycrystalline structure.

Thus it may be said that although the dominant growth direction of spheroidal graphite seems to be along the c-axis of the hexagonal graphite crystal in external appearance, it is actually along the a-axis. This will be explained later.

Substructure of C/V Graphite

The TEM photograph and diffraction pattern of C/V graphite are presented in Fig. 8(a), (b). The SEM photograph corresponding to the TEM photograph is presented in Fig. 9. Diffraction patterns obtained from points of a ~ t are shown in the TEM photograph, Fig. 8(b). Although the spots from prism face of the hexagonal graphite crystal are observed at points of f, g and k, the (002) spots from basal planes are observed at all the other points. In other words, the electron is applied parallel to prism face at points of f, g and k, but applied parallel to basal planes at all the other points. Therefore it is sure that most of the surfaces of C/V graphite are the basal plane.

A clearer SEM photograph by EPMA is shown in Fig. 10. It is observed that C/V graphite is constructed of graphite tips and that each layer is parallel to the graphite surface and from diffraction patterns the tip's face is basal plane. Thus it can be supposed that C/V graphite has the polycrystal form and its dominant growth direction is along the a-axis similarly to spheroidal graphite.

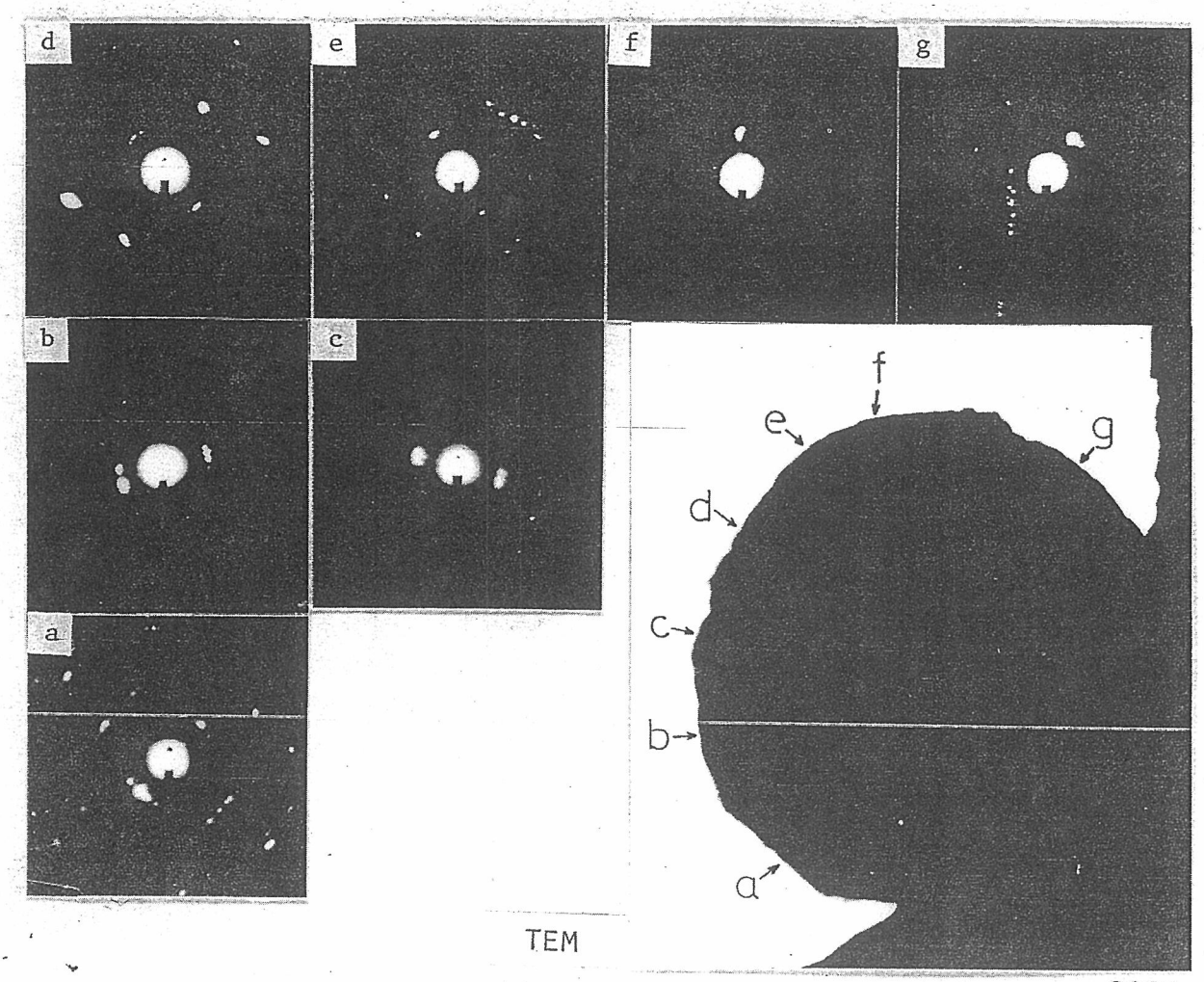

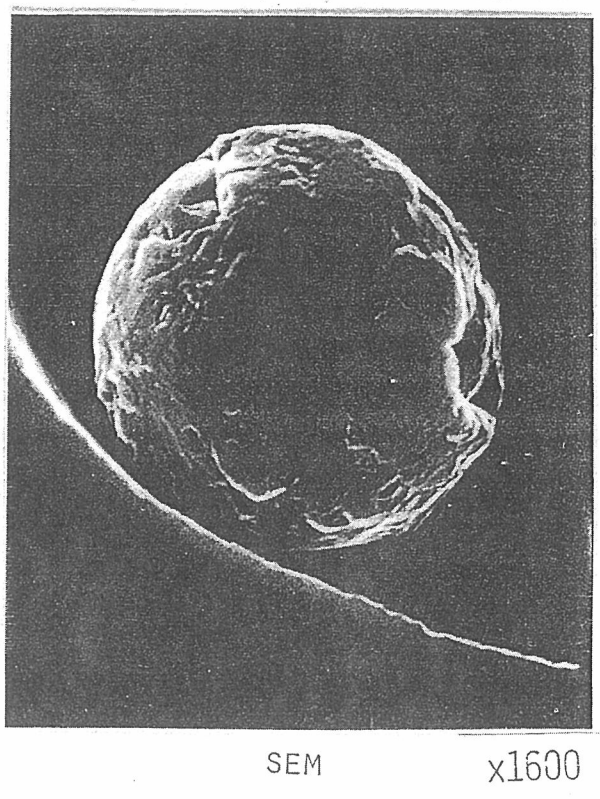

Fig. 6. TEM and SEM photograph and diffraction pattern of spheroidal graphite.

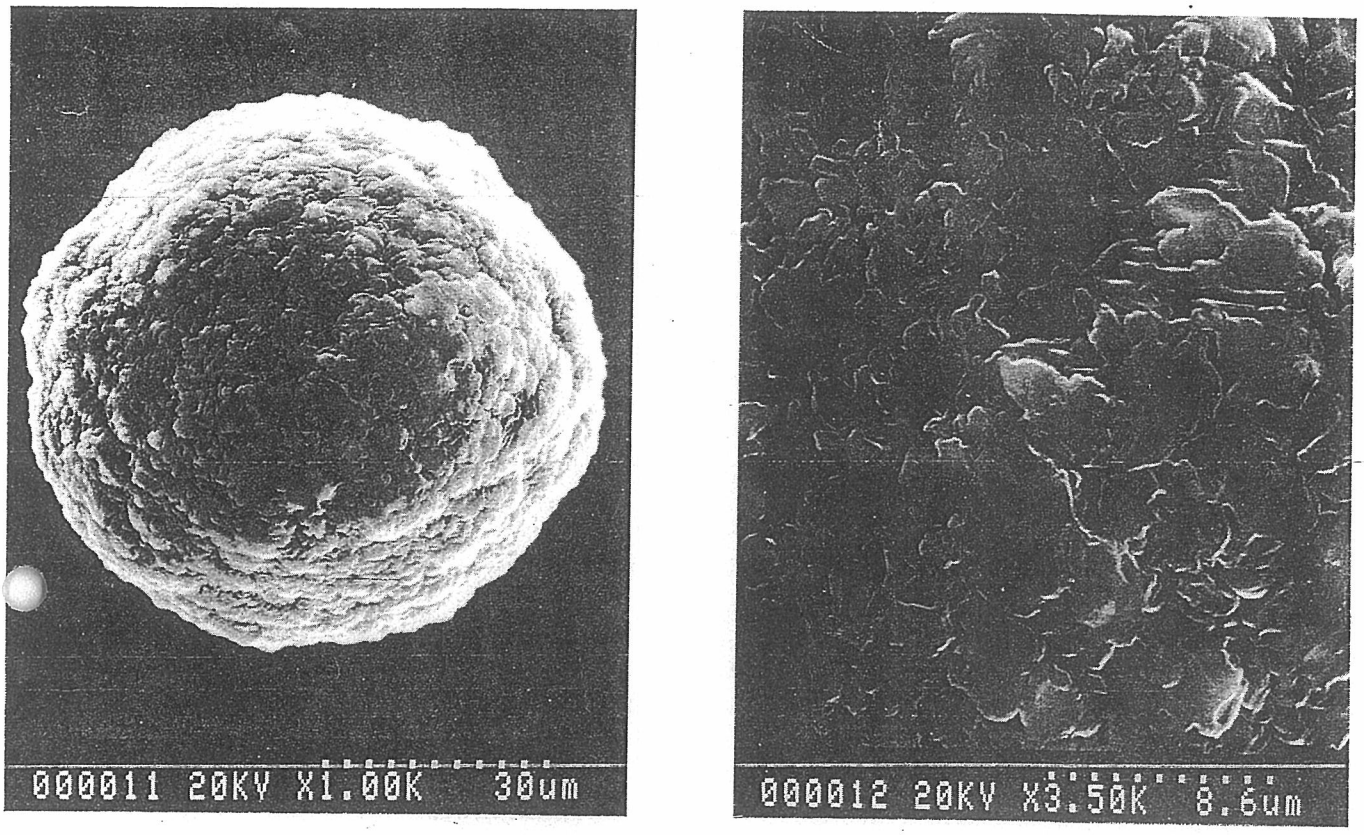

Fig. 7. SEM photograph of spheroidal graphite.

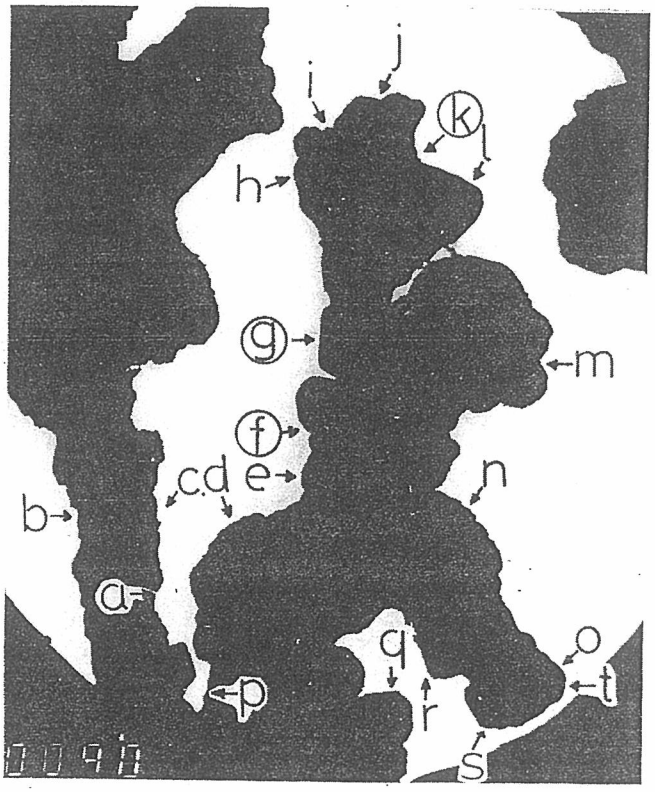

Fig. 8a. Diffraction patterns points a through t.

Fig. 8. TEM photograph and diffraction pattern of C/V graphite.

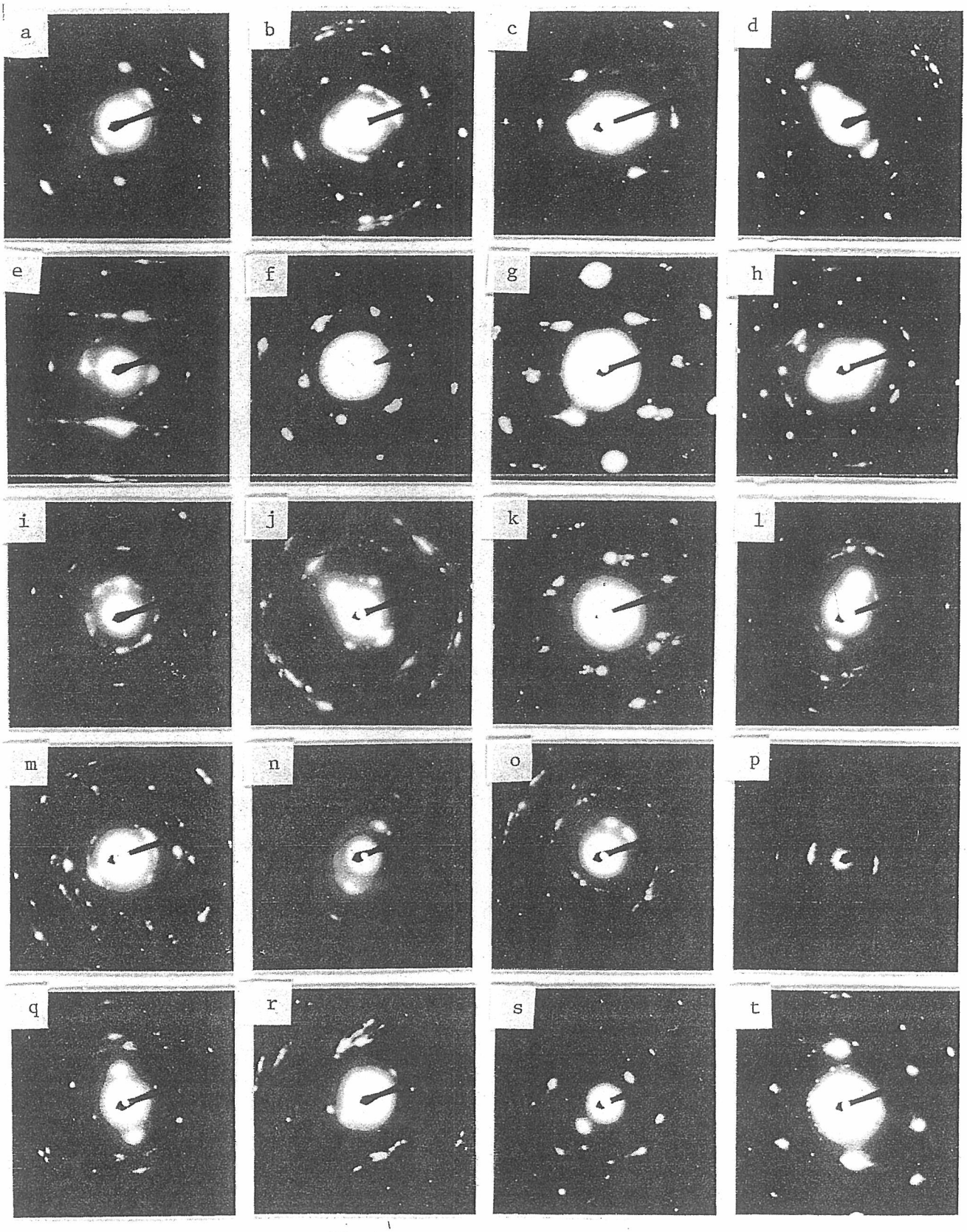

Fig. 8b. TEM photograph of C/V graphite.

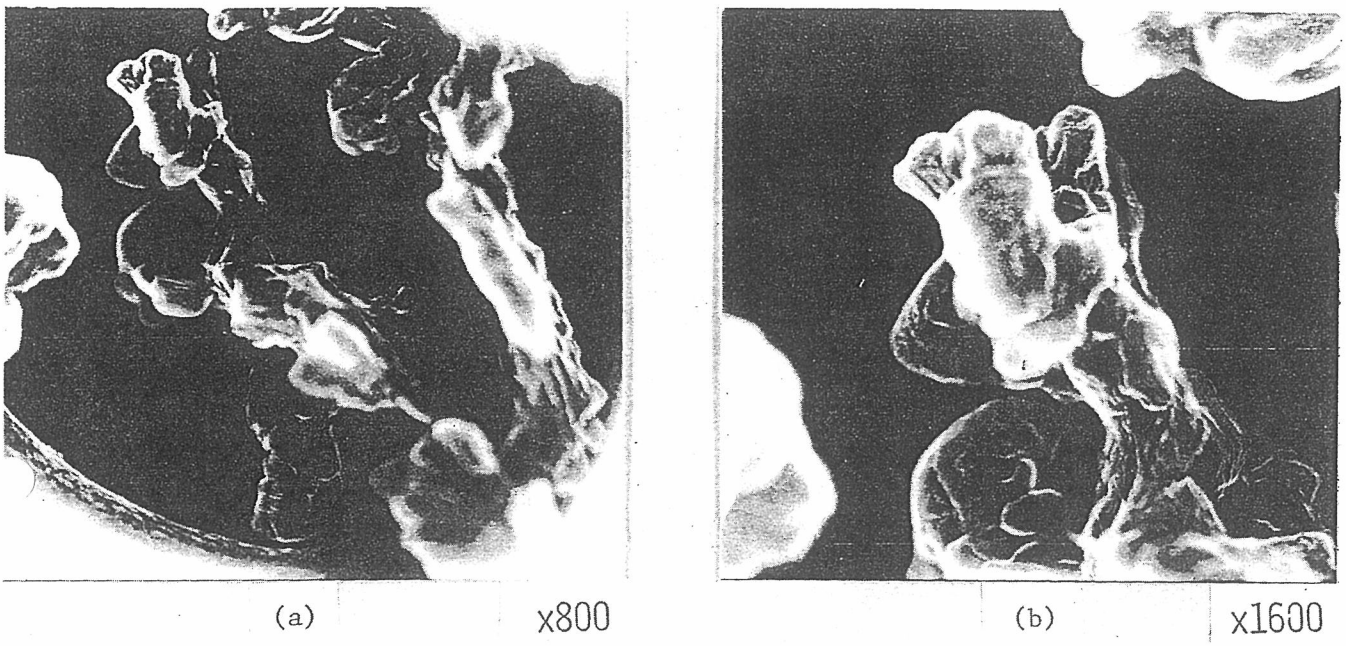

Fig. 9. SEM photograph of C/V graphite. These are the same graphite and view as presented in Fig. 8.

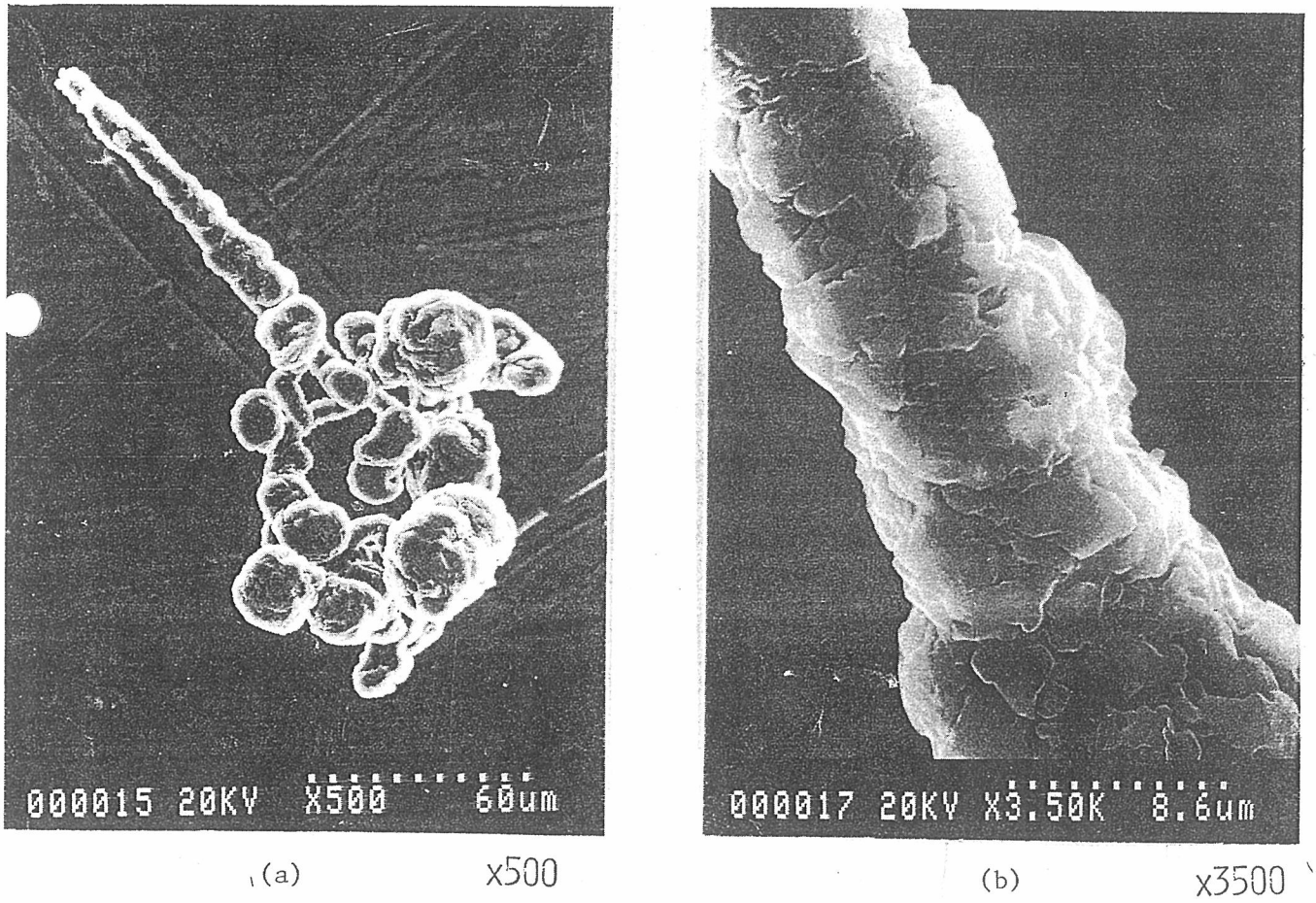

Fig. 10. SEM photograph of C/V graphite.

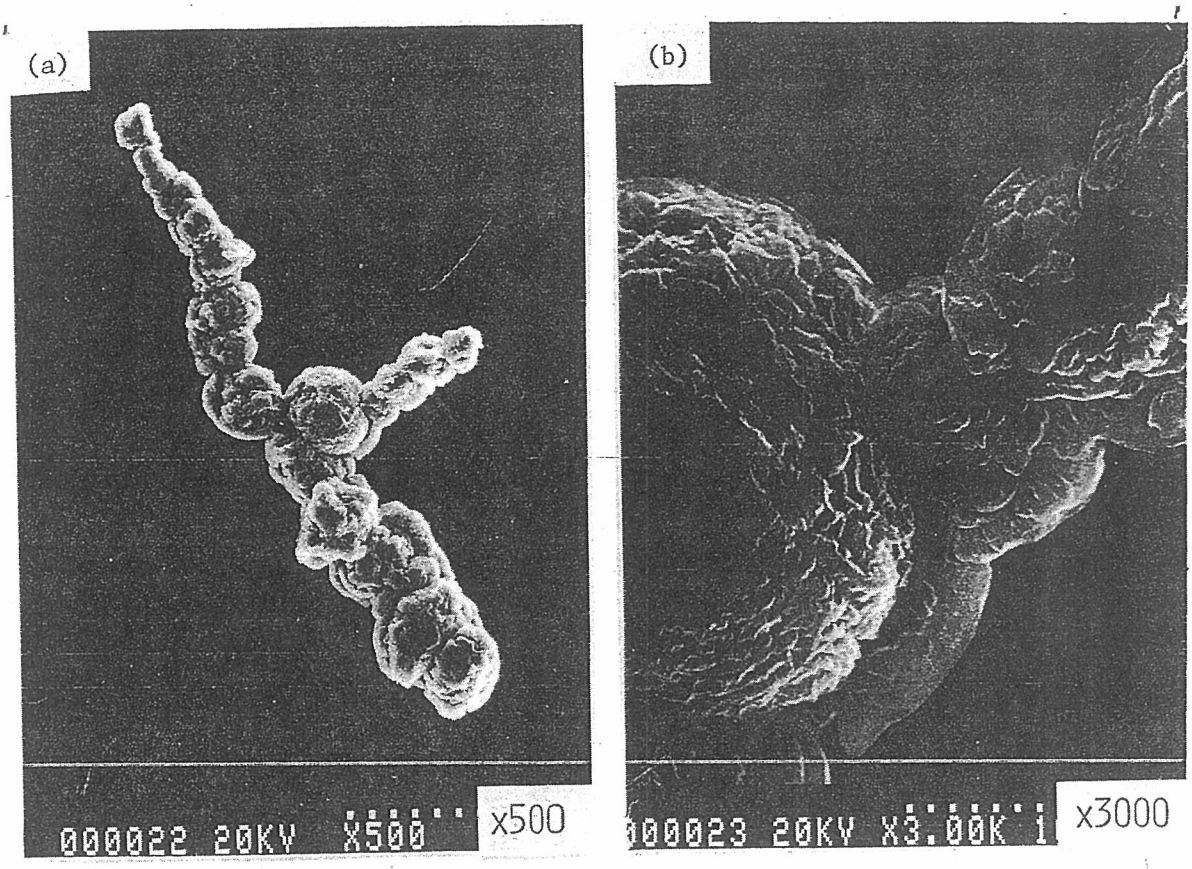

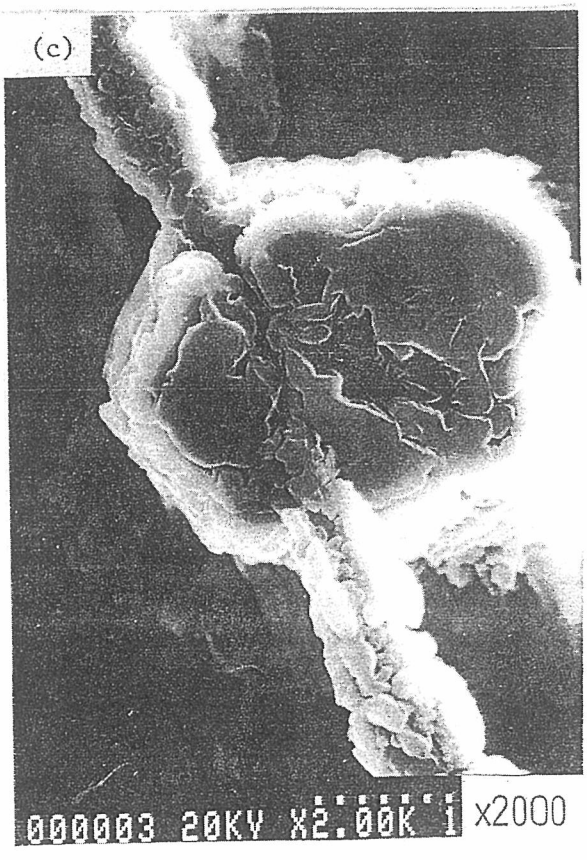

Fig. 11. SEM photograph of C/V graphite: a) and b) connected part between C/V and spheroidal graphite; c) branching of C/V graphite.

In addition, it has been frequently observed that spheroidal graphite is connected with C/V graphite in the graphite cell, shown in Fig. 11. This is the same result as re-polished examination in the former report.[1] The SEM photograph (by EPMA) of the connecting part between spheroidal and C/V graphite is presented in Fig. 11(a). It is predicted that neither graphite form has any structural relation wholly because the graphite tips are independently layered toward their surfaces. Figure 11(b) shows another example of connecting parts. It is observed that only connected parts may have some structural relation but there is no such relation at the other parts.

Figure 9(b) shows the parts where the only prism face was observed. It is supposed from this photograph that the graphite tips are layered to the same direction where the electron is applied. This situation is illustrated in Fig. 12. As the result of

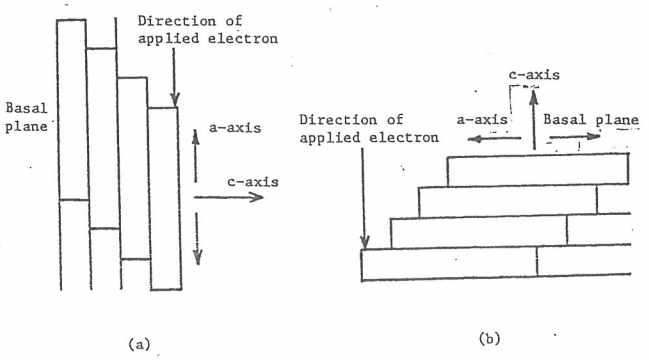

Fig. 12. Relationship of the direction between the applied electron and the graphite tip layers: a) case where the pattern from the basal plane is observed; b) case where the pattern from the prism face is observed.

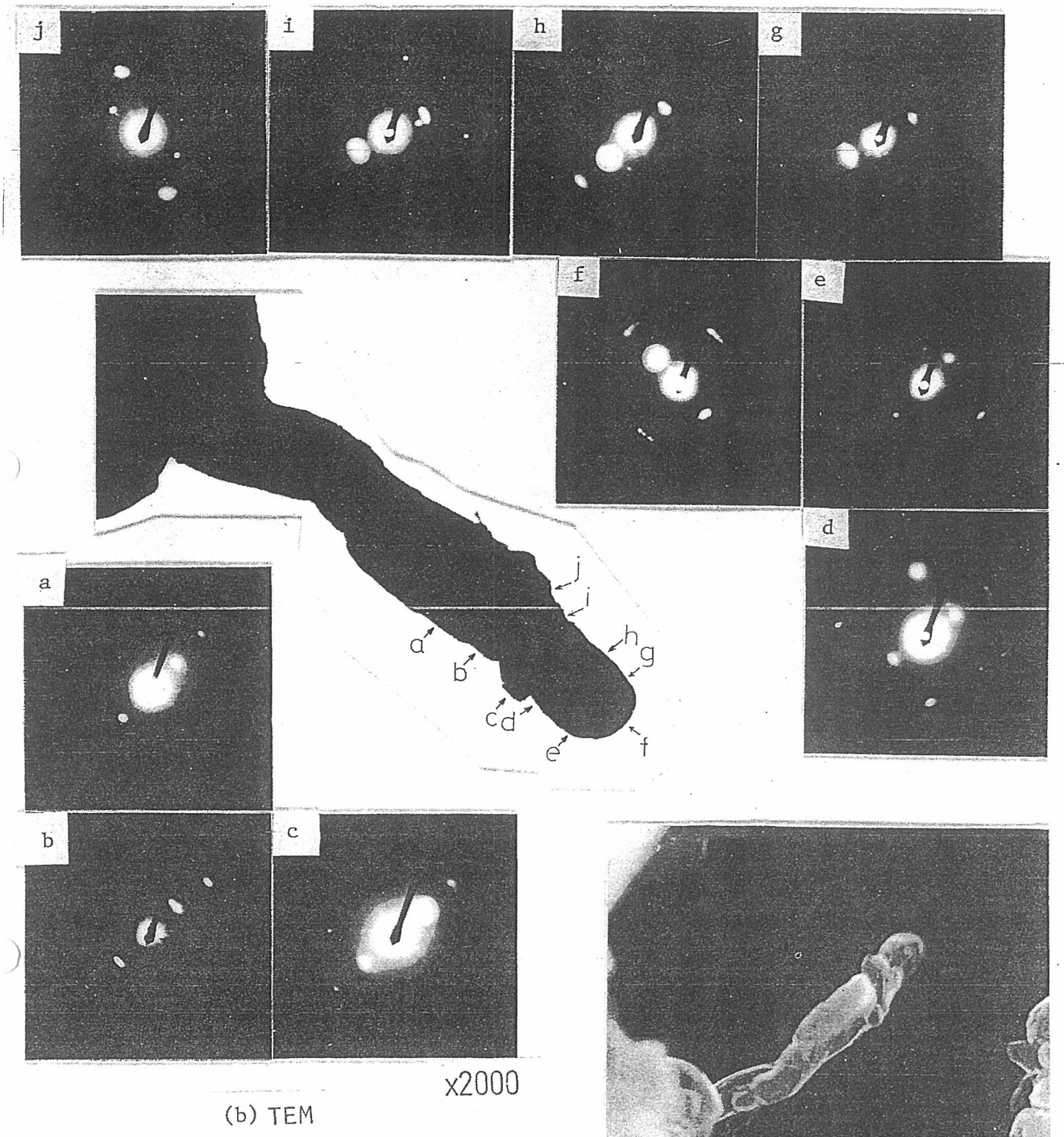

Fig. 13. Substructure of the C/V graphite end: a) SEM photograph; b) TEM and diffraction pattern photograph.

more examinations, it can be said that the diffraction patterns from the prism faces are observed at highly branched parts in the C/V graphite cell. The high branching may be a main reason why the prism face appeared on the surfaces.

The substructure of the C/V graphite end was observed at short intervals in detail. The results are presented in Fig. 13. The diffraction patterns show that the surface is covered with the basal plane and the c-axis directions are perpendicular to the every surface.

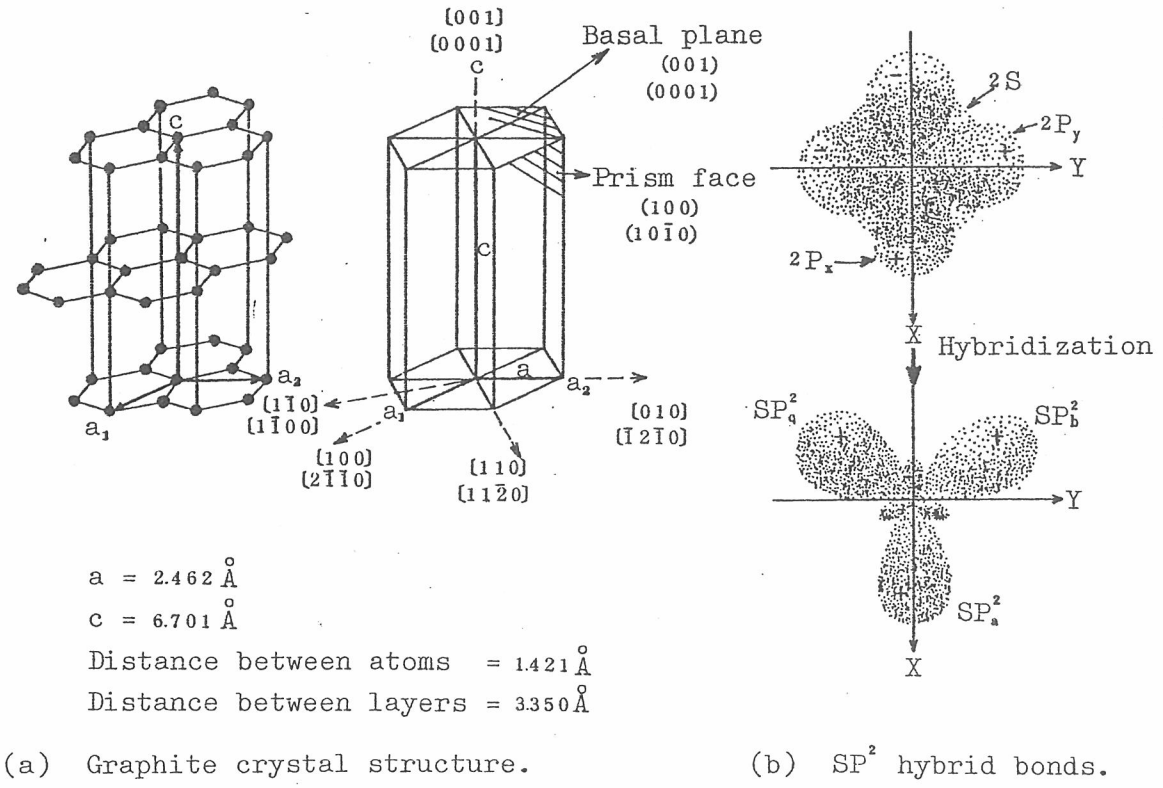

(a) Graphite crystal structure. (b) SP^2 hybrid bonds.

Fig. 14. Crystal structure and SP^2–σ Hybridization of graphite.

Thus it is supposed that C/V graphite has basically the same substructure as spheroidal graphite, although their shapes are different.

CONSIDERATION

As a result of observing several graphite substructures, it can be said that the dominant growth direction of graphite is always along the a-axis of hexagonal graphite structure, even if it takes any types of morphologies, although spheroidal and C/V graphite seem to grow along the c-axis in external appearance.

This can also be predicted from the crystal structure and nature of chemical bonding in graphite, shown in Fig. 14. The carbon atoms in the basal plane are bonded with a $SP^2 - \sigma$ hybridization, of which bonding energy is 70 thru 80 Kcal/mol.[5] On the other hand, the carbon atoms between the layers of the basal plane are bonded with a Van der Waals' force, of which bonding energy is about 4 Kcal/mol.[5] Thus the bonding energy of carbon atoms in the basal plane is much higher than that between the basal planes. Therefore it is predicted that graphite should grow dominantly along the a-axis of the hexagonal graphite structure, irrespective of graphite morphologies.

The authors believe that each type of graphite form depends on sites where the graphite is crystallized. This is explained by some examples as follows:

Kish Graphite

Kish graphite crystallizes and grows in the molten cast iron. Therefore, the dominant growth direction of the a-axis can be kept without any disturbance and graphite can be formed as a flat plate and single crystal.

Flake Graphite

Flake graphite crystallizes and grows together with austenite. Then, graphite is in contact with and extruded into the molten cast iron during the growth. The graphite growth is affected by austenite crystalline but the dominant growth direction of the a-axis is kept. Therefore, flake graphite may be highly branched and have the single plate crystal.

Spheroidal Graphite

Yamamoto[6,7] and Chang[8-15] have reported that the bubbles are introduced into the molten cast iron by the spheroidizer and that the diameter is below 10μ. The bubble is a free surface in the melt. Therefore graphite crystallizes into the bubbles easily. The process of graphite growth into the bubble is schematically illustrated in Fig. 15. At first, graphite crystallizes everywhere on a bubble's wall. Then each graphite tip grows along the bubble's wall and the growth direction is along a-axis. The growth along the a-axis is, however, stopped when the graphite tips collide with a neighboring tip. Since the solidification proceeds more and more, the growth along the c-axis is held momentarily until a certain unit of the basal plane is formed on the first basal plane. Then the growth along the a-axis is resumed on the first basal plane. Such growth is repeated and the bubble is filled up with the graphite tips. Thus, spheroidal graphite is formed.

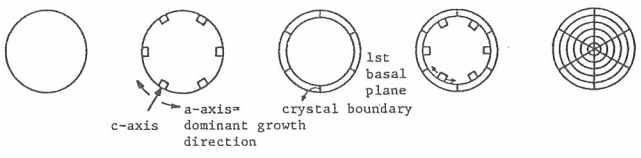

Fig. 15. Process of graphite growth into the bubble.

After spheroidal graphite is covered with an austenite shell, it is completely isolated from the melt. Then, the site where graphite crystallizes is provided by the diffusion of the iron atoms around spheroidal graphite through the austenite shell, as mentioned.[1] Therefore, spheroidal graphites grow outwardly as spheroidal graphite, in the same way as graphite grows in the bubbles but in the opposite direction.

C/V Graphite

As mentioned,[1] the growth of C/V graphite is the same as that of spheroidal graphite until graphite fills up the bubble as spheroidal graphites, but it differs after that. C/V graphite is in contact with the molten cast iron through filmy melt channels during the growth. Iron atoms diffuse mainly through the channels and graphite crystallizes along them. Although there is liquid at the channel, the dominant growth along the a-axes is limited within a certain size by the channel walls. Therefore it is supposed that the crystallization of C/V graphite at the channel proceeds in the same way as that of spheroidal graphite and both graphites have basically the same substructure.

SUMMARY

1) Although spheroidal and C/V graphite grow along the c-axis in external appearance, the dominant growth direction of both graphites is along the a-axis, in the same way as kish and flake graphite, as indicated by the nature of chemical bonding in the hexagonal graphite crystal.
2) All types of the graphite substructures depend on the site where graphite crystallizes.
3) The site for spheroidal graphite is the bubble at first and then it is transferred to the graphite-austenite shell interface. The site for C/V graphite is the bubble at first and then it is transferred to the filmy melt channel.
4) The graphite growth behavior is the same in the following cases:
   a) in the bubble, as illustrated in Fig. 15;
   b) at the channel;
   c) on the spheroidal graphite in the austenite shell. Therefore, spheroidal and C/V graphite have basically the same substructure and have the polycrystalline structure.
5) Spheroidal graphite exists as the original form of C/V graphite at early stages of the solidification. However, it does not affect the whole growth directly. Spheroidal graphite provides only sites where graphite crystallizes as C/V graphite.

REFERENCES

1. H. Itofuji, B. Chang, Y. Kawano, N. Inoyama, S. Yamamoto and T. Nishi, *AFS Transaction,* to be published.
2. T. Kimura, C. R. Loper, Jr. and H. H. Cornell, *AFS Transaction,* vol 89, p 359 (1981).
3. P. C. Liu, C. R. Loper, Jr., T. Kimura and E. N. Pan, *AFS Transaction,* vol 89, p 65 (1981.
4. N. N. Aleksandrov, B. S. Mil'man, N. G. Osada, L. V. Il'icheva and V. V. Andreev, *Russian Casting Production,* p 365 (Sep 1975).
5. R. O. Brenner, *Journal of Chemical Physics,* vol 20, p 40 (1952).
6. S. Yamamoto, B. Chang, Y. Kawano, R. Ozaki and Y. Murakami, *Metal Science,* vol 9, p 360 (1975).
7. S. Yamamoto, Y. Kawano, Y. Murakami, B. Chang and R. Ozaki, *AFS Transactions,* vol 83, p 217 (1975).
8. B. Chang, S. Yamamoto, Y. Kawano and R. Ozaki, *Imono,* vol 49, p 269 (1977).
9. B. Chang, S. Yamamoto, Y. Kawano and R. Ozaki, *Journal of the Japan Institute of Metals,* vol 41, p 464 (May 1977).
10. B. Chang, S. Yamamoto, Y. Kawano and R. Ozaki, *Journal of the Japan Institute of Metals,* vol 41, p 471 (May 1977).
11. B. Chang, S. Yamamoto, Y. Kawano and R. Ozaki, *Journal of the Japan Institute of Metals,* vol 41, p 479 (May 1977).
12. B. Chang, S. Yamamoto, Y. Kawano and R. Ozaki, *Journal of the Japan Institute of Metals,* vol 41, p 564 (June 1977).
13. B. Chang, S. Yamamoto, Y. Kawano and R. Ozaki, *Journal of the Japan Institute of Metals,* vol 41, p 571 (June 1977).
14. B. Chang, S. Yamamoto, Y. Kawano and R. Ozaki, *Journal of the Japan Institute of Metals,* vol 41, p 1019 (Oct 1977).
15. B. Chang, S. Yamamoto, Y. Kawano and R. Ozaki, *Journal of the Japan Institute of Metals,* vol 41, p 1025 (Oct 1977).